Supporting appendix

Supporting Text

Tables S1 to S5

Figures S1 to S8

References 1 to 37

1. Supporting text

Age-structured models

We applied two standard age-structured cohort models based on available information and parameters derived from previous studies and stock assessments for the Pacific sardine (1) and northern anchovy (2). The simulated population dynamics are represented by numbers-at-age (N) and biomass-at-age (B) distributed among 11 and 5 age classes for sardine (0 to 10+) and anchovy (0 to 4+), respectively, where the so-called plus group includes all fish 11 or 4 years and older. The following formulations regulate the population dynamics of sardine (Eq. 1) and anchovy (Eq. 2):

$$N_{a+1,\,t+1} = N_{a,\,t} e^{-(F_{a,\,t} + M)} \quad (1)$$

$$B_{a+1,\,t+1} = B_{a,\,t} e^{-(F_t + M - G)} \quad (2)$$

where $N_{a,t}$ and $B_{a,t}$ are the number or biomass-at-age a in year t, F the fishing mortality, M the natural mortality, i.e., fixed at 0.4 yr^{-1} and 1.06 yr^{-1} for sardine (1) and anchovy (3), respectively, and G the growth rate of anchovy set to 0.198 yr^{-1} (2). The SSB was estimated as the sum of the adult population given by the proportion of mature fish in each age class (1, 2, 4) and (in case of sardine) their corresponding mean weight-at-age (1). The models apply annual time steps, are

seasonally implicit and are assumed to be initiated at the time of spawning and recruitment for each species (5).

Introducing inter-specific competition

Although direct evidence of inter-specific competition is not supported by evidence and as such is considered unsubstantiated (6, 7), primarily based on the lack of negative correlation in SDRs (8), no significant cross-map signal between sardine and anchovy landings (9) and little niche overlap in terms of habitat and prey preference, i.e., due to different gill rake morphology and feeding modes (10, 11), we illustrated the management consequences if erroneously assuming species interactions to play a major role. To that end, we introduced inter-specific competition to the model by allowing the weight-at-age of sardine and growth rate (G) of anchovy to depend on the SSB of the competing species, based on the historical variation in anchovy weight by 54% derived from differences in scale widths in sediment records during periods of high and low sardine SDRs (12). Hence, we introduced a potential linear change in growth with a slope and intercept defined by an increase and decrease of 27% at low and high SSB, i.e., set to the 25^{th} and 75^{th} percentile of historical biomass estimates for sardine and anchovy (8, 12). Note that above and below these SSBs the growth may change even further, while at mean levels the parameters remain unchanged at their original values. Furthermore, we included an additional predation effect on 0-group sardine assuming that adult anchovy may significantly prey on sardine eggs and larvae (13) by allowing the natural mortality (M) of 0-group sardine to increase 25% at periods of high anchovy biomass.

Using this alternative parameterization, we evaluated whether the previously suggested reduction fishery of anchovy (14) would have enhanced recovery of the sardine during a 20-year period following its collapse in the 1950s. We performed multiple stochastic simulations over a range of fishing mortalities (i.e., anchovy F from 0 to 1 and sardine F set to 0) and estimated the mean SSB of anchovy and sardine over the last 5 years of the simulation. The simulations were initialized at the observed SSB values in 1963 (1, 2) and run for 20 years until 1982 forced with observed SST conditions (Fig. S7).

Stock-recruitment models

The recruitment process was implemented through environmentally-sensitive stock-recruitment (S-R) relationships based on previous studies on recruitment dynamics of Pacific sardine (15, 16) and Northern anchovy (17). Although a number of different models and approaches may be used to examine stock-recruitment relationships, we applied the same nonlinear regression techniques, i.e., Generalized Additive Models (GAMs) (18, 19), as previously used to examine the effect of parental population size (SSB) and environmental forcing on recruitment dynamics of sardine and anchovy. Although the distribution of sardine and anchovy may range from Canada to Baja California (20), especially during periods of high abundance, the annual mean 5-15m temperature (here also termed Sea Surface Temperature (SST)) from the regular California Cooperative Oceanic Fisheries Investigations (CalCOFI) area (i.e., averaged over all stations sampled over the entire period on lines 76.7 to 93.3) was chosen as the single environmental variable as it proved the most significant predictor affecting recruitment during model selection (16) (Table S1-S2). Furthermore, the area covers a large part of the main spawning area of

Pacific sardine and northern anchovy in the southern California Bight (21, 22). The following linearized formulations with log-transformed recruitment (R) estimates as responses were used:

$$\ln(R)_t = a + s(SSB_t) + s(SST_t) + \varepsilon \quad (3)$$

where a is the intercept, s the thin plate smoothing function (23), and ε the Gaussian error term. In contrast to previous studies on sardine recruitment (15, 16), the S-R model was refitted using R at age 0 rather than R at age 2. The model for Northern anchovy was based on R at age 0 as previously used (2, 17). The S-R models were fitted on available time series of R, SSB and SST covering the same time period from 1981-2010. During model fitting the degrees of freedom of the spline smoother function (s) was constrained to three knots (k=3) to allow for potential nonlinearities, but also restrict flexibility.

We applied a model reduction routine based on Generalised Cross Validation (GCV) and partial F-tests to test for the best set of predictors (Table S4). In addition, we performed a cross validation analysis by fitting the final models to a randomly selected subset of the data (24), i.e., amounting to 75% of the observations, and assessed the predictive accuracy of the models by comparing the observed values with the predicted recruitment estimates for the remaining subset. The cross-validation analysis was repeated 1000 times (i.e., with new random draws each time) in order to assess the range of uncertainty associated with the predictions.

Climate module

While observed SST values were used for model fitting and validation, as well as management simulations regarding the sardine collapse during the 1950s (Fig. 2A-B), surrogate time series of SST were used as input only during long-term model simulations. Since marine climate is generally positively autocorrelated (25), we used a $1/f^{\beta}$ climate module able to generate "red-shifted" noise accurately resembling the natural variability of the observed SST time series, i.e., based on estimating the spectral exponent (beta) of a model fitted to the power spectrum in log coordinates (26-28). Hence, the surrogate SST time series display the same relative distribution of frequencies, i.e., the same slope (beta) of the Fourier spectrum, as the original SST time series used during model fitting. The slope was estimated based on the log-transformed power spectrum with a robust linear regression procedure using iterated re-weighted least squares (function ''rlm'' from the package MASS in the statistical software R).

Recreating decadal-scale population dynamics

The first validation exercise hindcasted the population dynamics of sardine and anchovy over the time period corresponding to available stock assessments during 1981-2010 (1) and 1963-1991(2), respectively. The simulations were initialized based on observed numbers- and biomass-at-age in 1981 and 1963 and run forward forced by observed SST conditions and estimated F values from each respective stock assessment. Note that while age-specific F values were available for sardine (1), F values for anchovy F values were assumed constant across ages (2). The predictive accuracy of the hindcast was assessed by comparing the mean and range of

the simulated SSB dynamics with observed SSB estimates from the corresponding stock assessments (Fig. S4).

Recreating multi-decadal-scale population dynamics

The second validation exercise aimed to recreate the multi-decadal dynamics of sardine and anchovy throughout a longer period (from 1935 onwards), not consistently covered by stock assessments. As starting values for sardine numbers-at-age derived from previous stock assessments (6) were used, while in the absence of stock assessment estimates for anchovy these simulations were initialised at mean historic biomass-at-age (2). Then, the model was run forward based on observed SSTs and landings available throughout the period. Since CalCOFI SST records are available only from 1949 onwards, although scattered and including missing values, we extended the time-series until 1935 using reconstructed SST, based on the NOAA_ERSST_V3 (29) extracted for the CalCOFI area. Note also that in the absence of F stock assessment estimates throughout most of the period, we introduced a fishing effect by reducing the population sizes with the observed landings reported for sardine and anchovy in each corresponding year. As previously performed, the predictive accuracy of the hindcast was assessed by comparing the simulated SSBs with observed SSB estimates (Fig. 1B).

Recreating centennial-scale population dynamics

The third validation exercise aimed to recreate the centennial-scale population variability of sardine and anchovy, illustrated by fish scale-deposition rates (SDR) from the Santa Barbara

Basin covering the last two millennia (8, 30). In order to hindcast the population dynamics of sardine and anchovy, we compiled and compared a number of available indices of regional climate variability to force the population dynamics during this period (31-36). Although considered as reconstruction of the Pacific Decadal Oscillation (PDO) the indices differ considerably, especially prior to 1900 (Fig. S8). We used the linear relationship between CalCOFI SST and the regional climate indices during the overlapping time period to extend the input SST time series backwards in time (Table S5). Since the SDRs of sardine and anchovy are based on 10-year averages we assessed the predictive accuracy of each hindcast as the correlation between ln(SDR+1) and 10-year averages of ln(SSB) (Table S5). The best climate proxy, demonstrating the highest correlation between simulated SSB and SDRs for both sardine and anchovy, was derived as the first-principle component of tree ring growth widths in the S. California/Baja California area (35). Note that due to uncertainty in dating the SDRs, i.e., an overall chronological offset of 50 years occur near the midpoint of the series (8), and hence a potential discrepancy in the timing of SDRs and the simulated population dynamics, highest correlations were found with a lag of 10 years (Fig. 1C).

Recreating the observed time-scales of variability (Fourier spectra)

In addition to the validation exercises, we performed an analysis comparing the Fourier spectra of long-term population dynamic simulations with the observed time scales of variability from the SDRs (8, 28). Hence, we performed multiple stochastic simulations over a time period of 1000 years, i.e., based on replicate SST time series accurately resembling the natural variability (variance spectra) of observed SST (e.g., Fig. 1D), computed 10-year averages of the output SSB

and derived the corresponding power spectra for each species and run after having filtered out the lower frequency variability (i.e., periodicity > 150 years) (8) using a spline smoother (i.e., GAM with k=20). Note that due to the coarse ten-year sample resolution of original SDRs, this analysis does not allow for a reliable comparison at higher frequencies (i.e., periods below 30 years) (8).

2. Supporting tables and figures

Table S1. Climate covariates used during sardine recruitment model fitting.

Variable	Month	Area	Source
SST_SIO_spring	March-May	SIO pier	http://www.shorestation.ucsd.edu/
SST_SIO_ann	Annual	SIO pier	http://www.shorestation.ucsd.edu/
SST_spring	March-May	CalCOFI	http://calcofi.org/data.html
SST_ann	Annual	CalCOFI	http://calcofi.org/data.html
ERSST_spring	March-May	CalCOFI	ftp://ftp.ncdc.noaa.gov/pub/data/cmb/ersst/
ERSST_ann	Annual	CalCOFI	ftp://ftp.ncdc.noaa.gov/pub/data/cmb/ersst/
ERSST_CCE_ann	Annual	CCE*	ftp://ftp.ncdc.noaa.gov/pub/data/cmb/ersst/
ERSST_CCE_spring	March-May	CCE*	ftp://ftp.ncdc.noaa.gov/pub/data/cmb/ersst/
ERSST_SBC_ann	Annual	S. Baja California *	ftp://ftp.ncdc.noaa.gov/pub/data/cmb/ersst/
ERSST_SBC_spring	March-May	S. Baja California *	ftp://ftp.ncdc.noaa.gov/pub/data/cmb/ersst/
PDO_spr	March-May	----	http://jisao.washington.edu/pdo/PDO.latest
PDO_ann	Annual	----	http://jisao.washington.edu/pdo/PDO.latest
MEI_spr	March-May	----	http://www.esrl.noaa.gov/psd/enso/mei/
MEI_ann	Annual	----	http://www.esrl.noaa.gov/psd/enso/mei/

* The selected areas reflect the entire spawning area in the California Current Ecosystem (CCE), as well as the southern spawning area off Baja California (20)

Table S2. The generalized cross validation scores (GCV), deviance explained (DEV) and p-values of the climate effect after fitting the GAM stock-recruitment models to each covariate separately. For each variable, annual (ann) and spring (spr) means, as well as three year averages (denoted by 3) were investigated. P-values have been modified for multiple hypotheses testing (37). (The best models are shown in bold).

Variable	GCV	DEV	p
SST_SIO_spring	0.643	0.604	0.006
SST_SIO_ann	0.792	0.527	0.156
SST_spring	0.762	0.536	0.094
SST_ann	**0.533**	**0.676**	**0.001**
SST_SIO_spr_3	0.735	0.572	0.055
SST_SIO_ann3	0.812	0.536	0.23
SST_spr_3	0.83	0.498	0.378
SST_ann3	0.801	0.512	0.212
PDO_spr	0.766	0.533	0.103
PDO_ann	0.85	0.482	0.514
MEI_spr	0.657	0.599	0.013
MEI_ann	0.744	0.545	0.059
PDO_spr3	0.865	0.473	0.944
PDO_ann3	0.865	0.473	0.958
MEI_spr3	0.765	0.534	0.106
MEI_ann3	0.722	0.587	0.06
ERSST_ann	0.719	0.587	0.062
ERSST_ann3	0.853	0.48	0.648
ERSST_spr	0.79	0.537	0.183
ERSST_spr3	0.856	0.478	0.664
ERSST_CCE_ann	0.718	0.561	0.034
ERSST_CCE_ann3	0.712	0.59	0.036
ERSST_CCE_spr	0.663	0.595	0.013
ERSST_CCE_spr3	0.728	0.574	0.037
ERSST_SBC_ann	0.745	0.543	0.05
ERSST_SBC_ann3	0.702	0.602	0.044
ERSST_SBC_spr	0.671	0.588	0.012
ERSST_SBC_spr3	0.716	0.576	0.052

Table S3. Summary statistics of parametric coefficients and smooth terms for the final stock-recruitment model for Pacific sardine (R_s) and northern anchovy (R_a).

A. Intercept

Response	Estimate	SE	t-value	p-value
$\ln(R_s)$	14.80	0.14	104.3	<0.001***
$\ln(R_a)$	12.54	0.14	123.3	<0.001***

B. Smooth terms

Response	Predictor	edf	F-value	p-value
$\ln(R_s)$	SSB	1.97	31.89	<0.001***
$\ln(R_s)$	SST	1.47	11.47	<0.001***
$\ln(R_a)$	SSB	1.89	18.30	<0.001***
$\ln(R_a)$	SST	1.00	7.92	0.01**

*edf is the estimated degrees of freedom for the model smooth terms where edf>1 indicates a non-linear relationship

Table S4. Model selection based on likelihood ratio tests and GCV scores for Pacific sardine (R_s) and northern Anchovy (R_a). The total deviance explained (DEV in %) and the significance of the likelihood ratio test (p) are shown. The final models are highlighted in bold.

Nr.	Model	GCV	DEV(%)	p
1.	$\ln(R_s) \sim \alpha + s(SSB) + \varepsilon$	1.05	60.8	
2.	$\mathbf{\ln(R_s) \sim \alpha + s(SSB) + s(SST\_ann) + \varepsilon}$	**0.69**	**77.2**	**<0.001**
1.	$\ln(R_a) \sim \alpha + s(SSB) + \varepsilon$	0.39	61.1	
2.	$\mathbf{\ln(R_a) \sim \alpha + s(SSB) + s(SST\_ann) + \varepsilon}$	**0.32**	**70.9**	**0.01**

Table S5. PDO reconstruction used as SST proxies during centennial-scale model hindcasts. The explained variance (R^2) and number of observations (N) of linear relationships between CalCOFI SST and each PDO reconstruction, as well as the correlation (Pearson´s r) between simulated biomass and SDRs for sardine (s) and anchovy (a) are shown. (The best predictor is highlighted in bold).

PDO reconstruction	Reference	Start year	R^2	N	r_s	r_a
Gedalof and Smith (2001)	31	1600	0.01	33	0.09	0.25
Darrigo et al. (2001)	32	1700	0.12	29	-0.26	0.65
MacDonald and Case (2006)	33	993	0.76	46	-0.22	-0.16
Darrigo and Wilson (2006)	34	1565	0.43	54	0.25	-0.04
Biondi et al. (2001)	**35**	**1661**	**0.4**	**41**	**0.55**	**0.85**
Shen et al. (2006)	36	1470	0.47	48	0.35	0.30

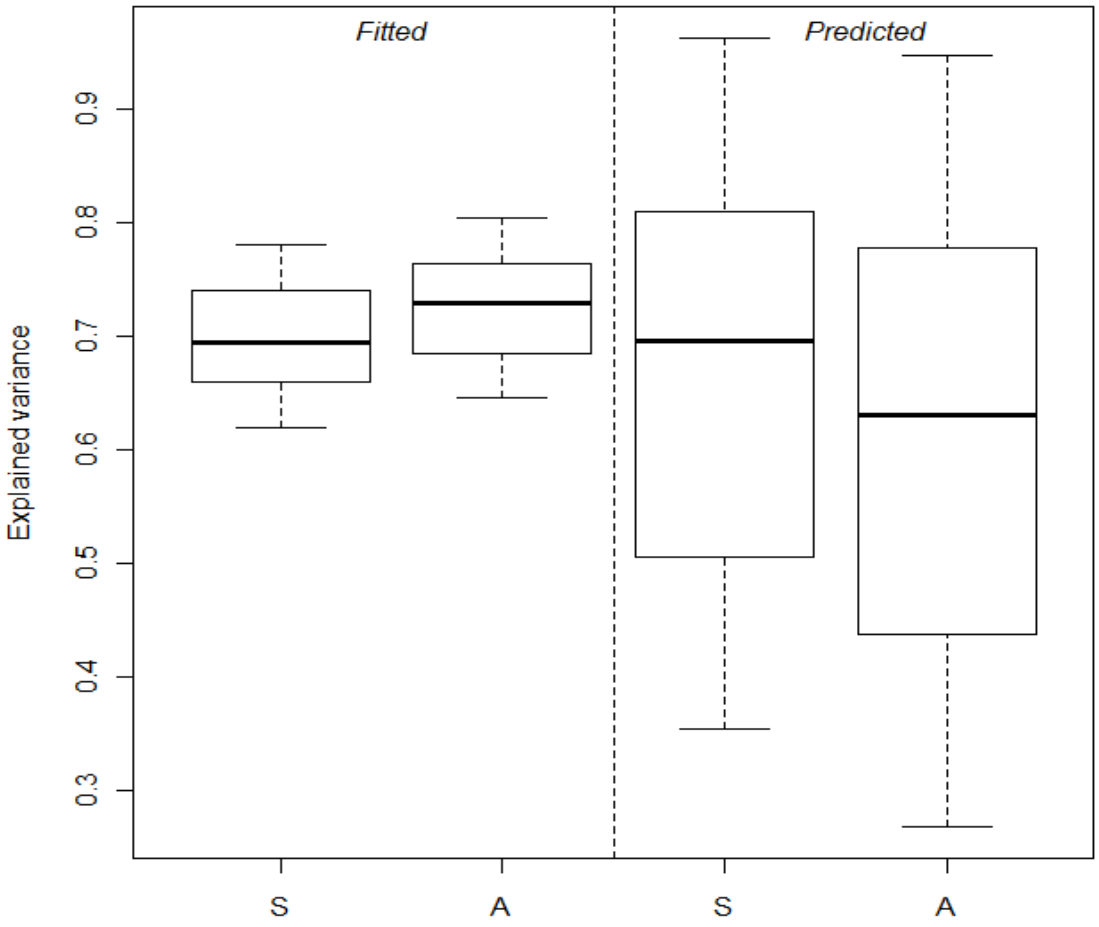

Fig. S1. Boxplots of explained variance from a cross-validation analysis of S-R model fit on a randomly selected subset for sardine (S) and anchovy (A), as well as the associated accuracy of recruitment predictions on the remaining data.

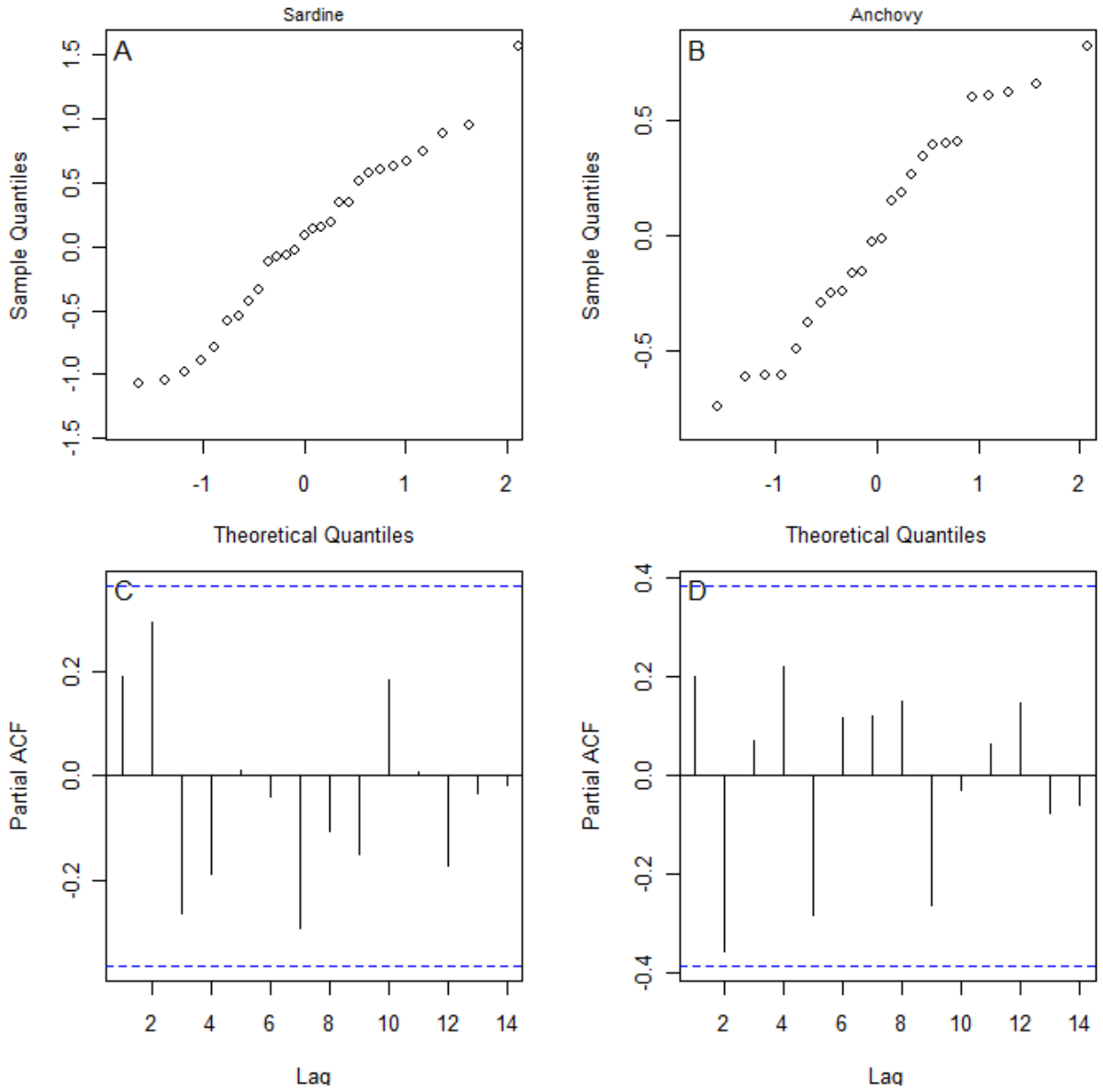

Fig. S2. Normal probability plots (A, B) and partial autocorrelation plots (C, D) of the final S-R models for sardine (left) and anchovy (right).

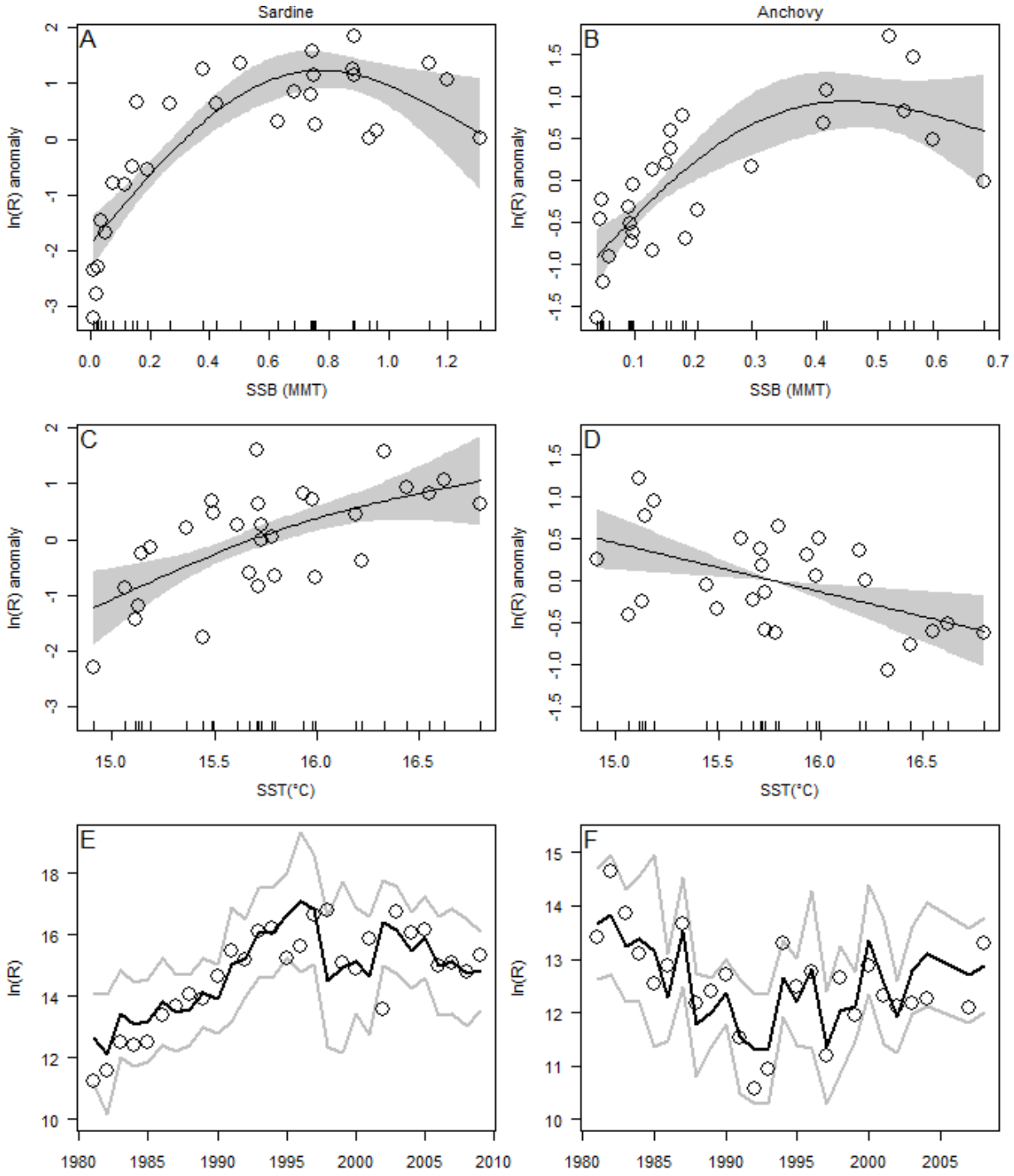

Fig. S3. Final smooth terms of S-R models for sardine (left) and anchovy (right) demonstrating the relationship between *R*, SSB (A, B) and SST (C, D). In panels (E, F) observed (circles) and modelled recruitment estimates are shown with upper and lower 95% confidence intervals (grey).

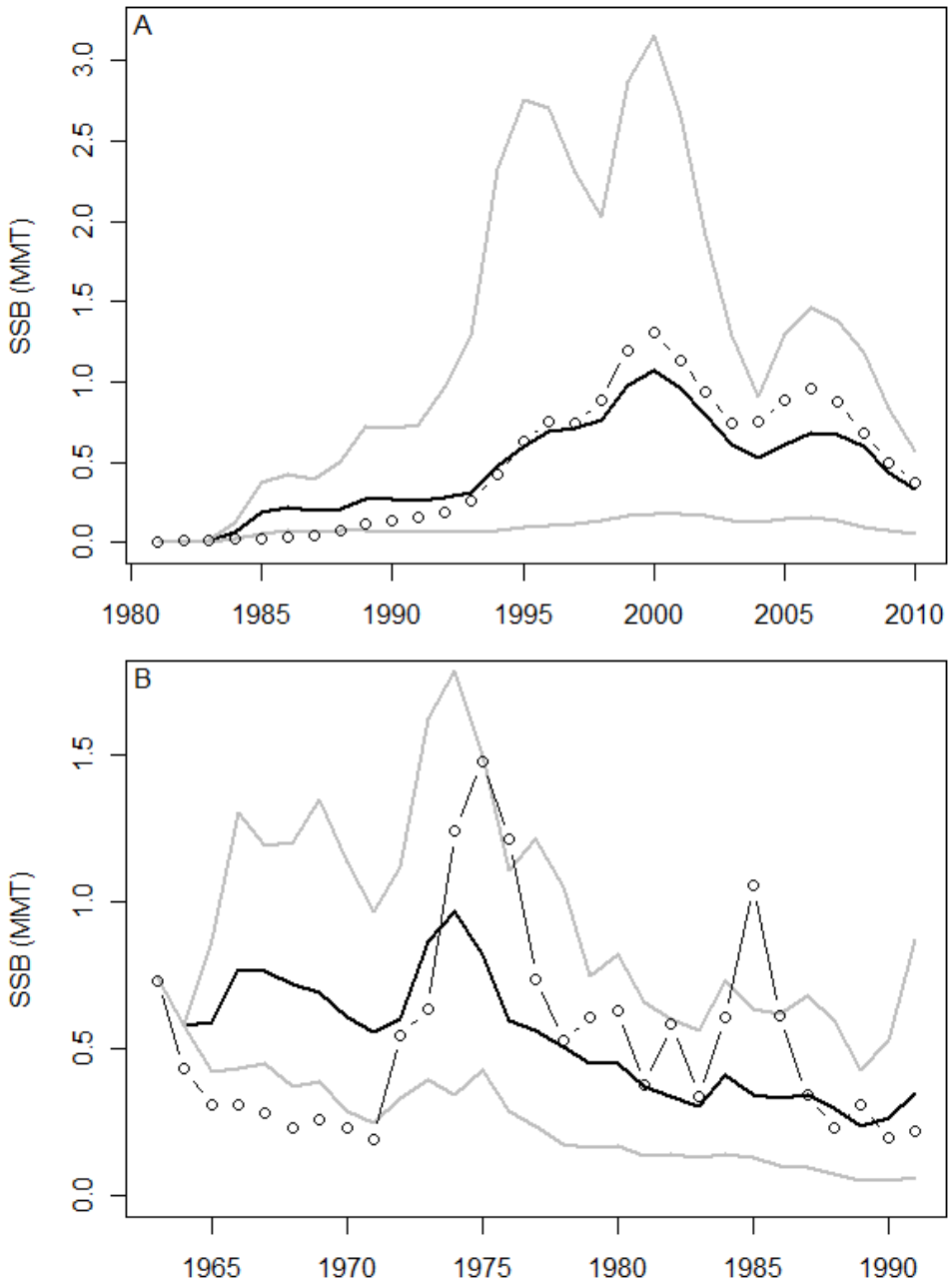

Fig. S4. Hindcast simulations of sardine (A) and anchovy (B) spawning stock biomass (SSB) initiated at estimated numbers- and biomass-at-age and projected forward based on observed climate condition (SST) and F-values. Simulated SSB (black) are shown with upper and lower 95% confidence intervals (grey), i.e., based on adding randomly resampled residuals from the S-R models, while observed SSB estimates are illustrated by circles.

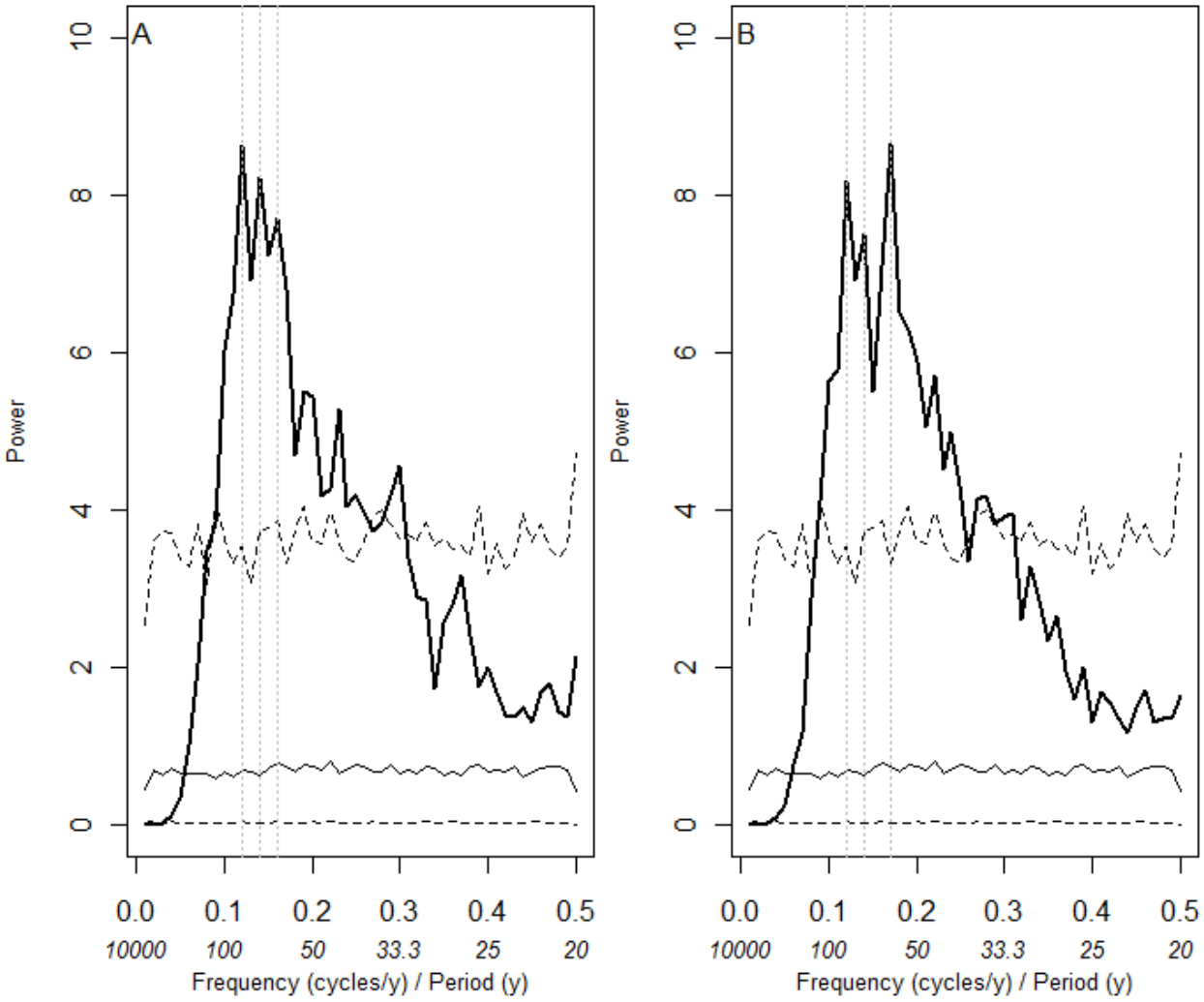

Fig. S5. Power spectra of sardine (A) and anchovy (B) SSB based on multiple stochastic simulations relative to the distribution of Gaussian (white) noise. (Mean and 95% confidence intervals are shown by horizontal solid and dashed lines, respectively). Significant frequencies, corresponding to periodicities based on SDRs (8) are show by vertical dashed lines.

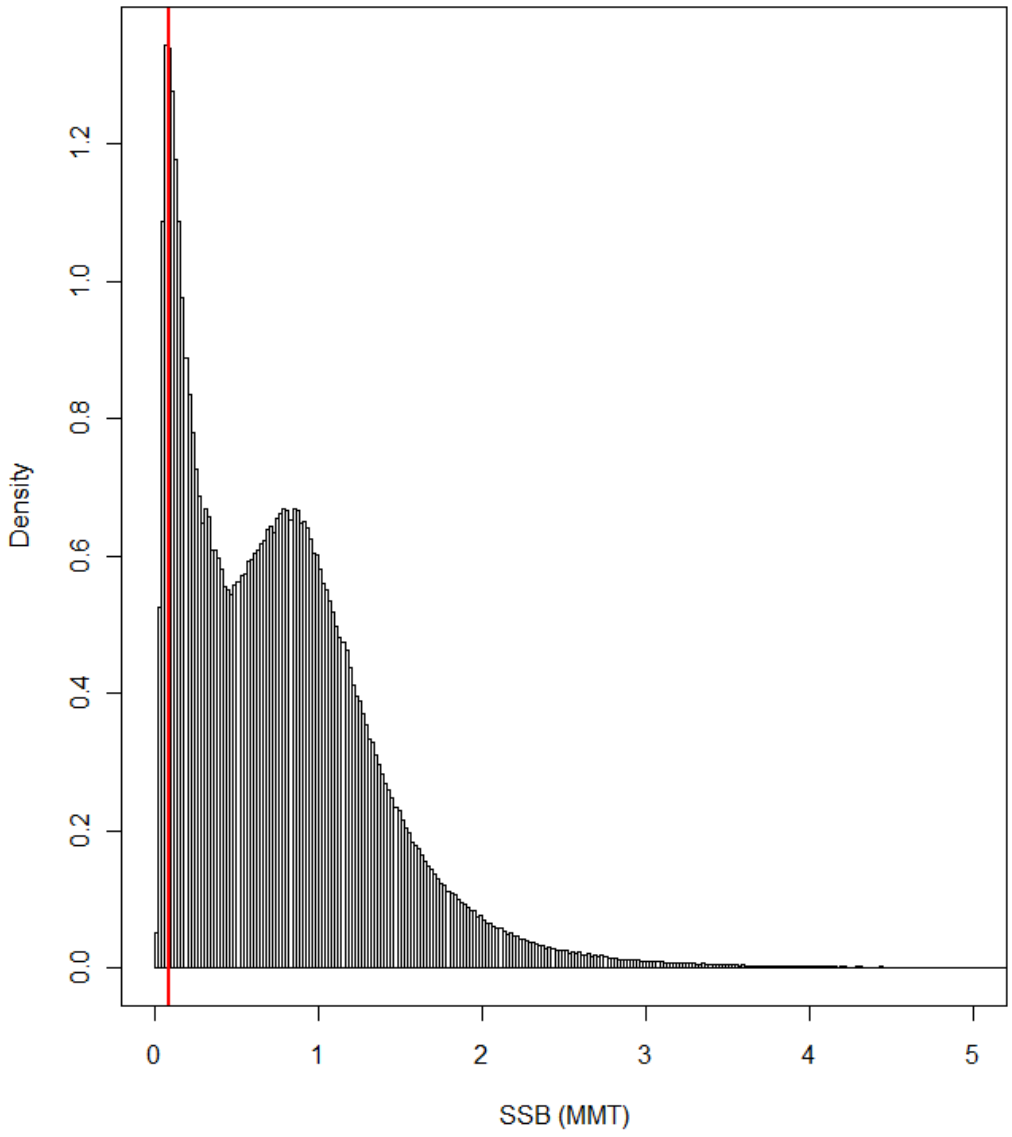

Fig. S6. Histogram of sardine SSB after multiple long-term simulations (i.e., 1000 stochastic simulations each spanning 1000 years; e.g., Fig. 1D) without fishing and climate (SST) fluctuating at mean historical levels. The red vertical line indicates the most frequently occurring minimum SSB of the lower mode of the bimodal distribution (0.09 MMT), below which the stock is considered as collapsed.

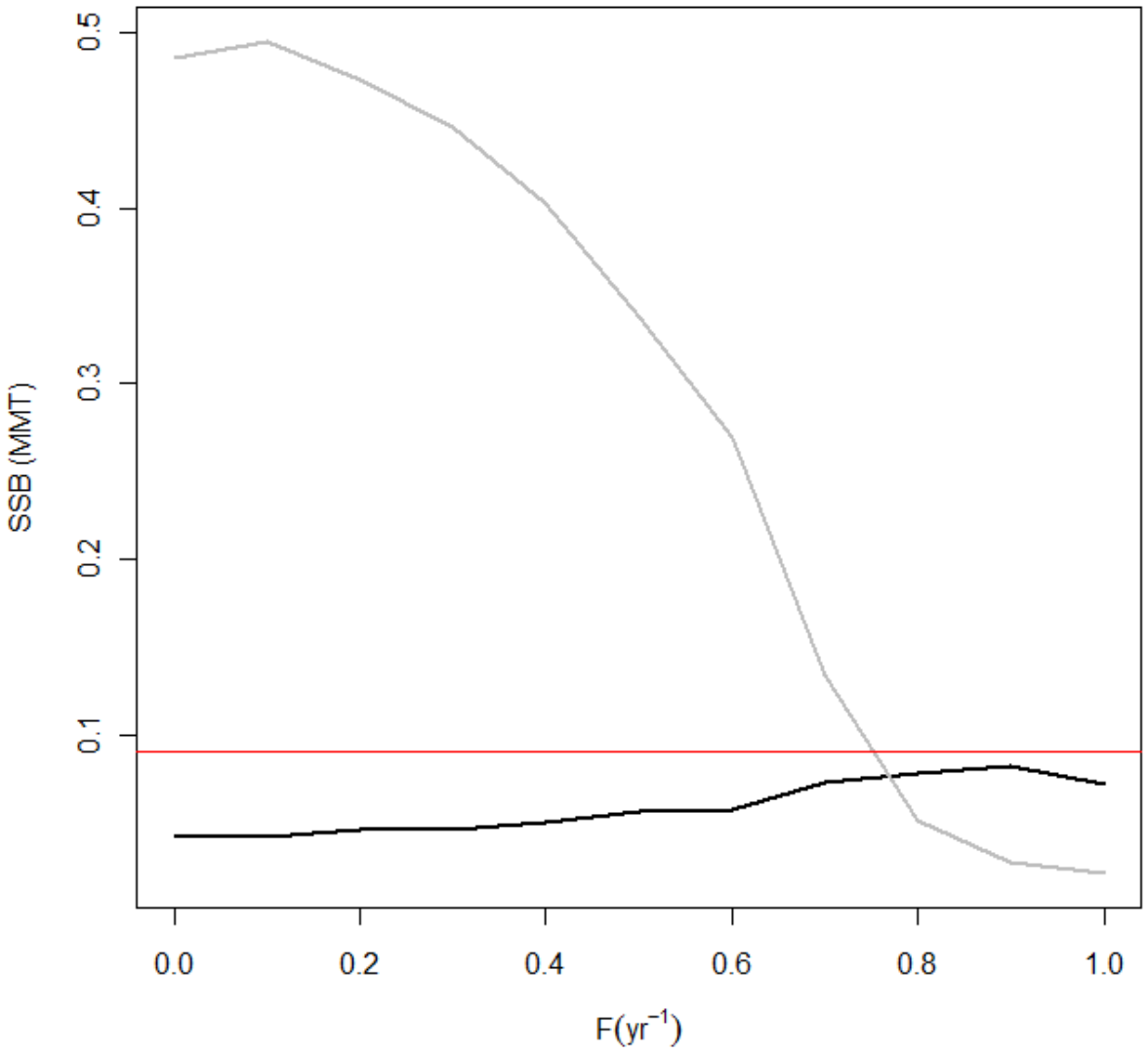

Fig. S7. Management simulations if erroneously assuming species interactions and introducing a reduction fishery on anchovy as a management strategy for sardine recovery following its collapse in the 1950s. The mean SSB of anchovy (grey) and sardine (black) over the last 5 years of the simulation (based on 1000 stochastic runs) over a range of fishing mortalities (i.e., anchovy F from 0 to 1 and sardine F set to 0). The simulations were initialized at the observed SSB values in 1963 and run for 20 years until 1982 forced with observed SST conditions. The red horizontal line indicates the minimum stock size (0.09 MMT) below which the sardine stock is considered as collapsed.

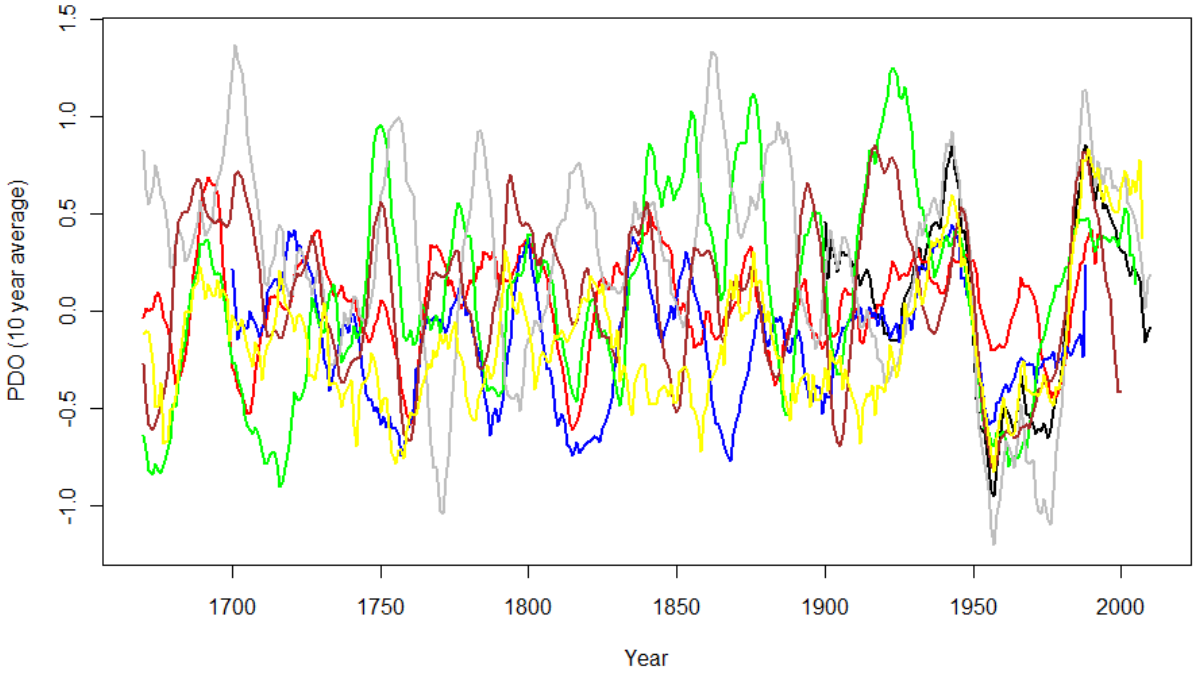

Fig. S8. Long-term dynamics of a number of PDO reconstructions (shown as 10 year running averages) where the black line denotes the PDO and the red (31), blue (32), green (33), grey (34), brown (35) and yellow (36) lines PDO reconstructions.

3. Supporting references

1. Hill K, Lo N, Macewicz B, Crone PR, Felix-Uraga R (2010) *Assessment of the Pacific sardine resource in 2010 for U.S. management in 2011*. (U.S Department of Commerce, La Jolla).

2. Jacobson L, Lo N, Barnes J (1994) A Biomass-Based Assessment Model for Northern Anchovy, *Engraulis mordax*. *Fish Bull* 92:711-724.

3. MacCall A (1974) The Mortality rate of *Engraulis mordax* in Southern California. *CalCOFI Rep* 17:131-135.

4. Peterman R, Bradford M, Lo N, Methot R (1998) Contribution of Early Life Stages to interannual Variability in Recruitment of Northern Anchovy (*Engraulis mordax*). *Can J Fish Aquat Sci* 45:8-16.

5. Checkley DM, Alheit J, Oozeki Y. Eds. (2009) *Climate Change and Small Pelagic Fish*. (Cambridge University Press, Cambridge).

6. Murphy GI (1966) Population biology of the Pacific sardine (*Sardinops caerulea*). *Proc Cal Acad Sci* 34:1-84.

7. MacCall AD (2009) *in: Climate Change and Small Pelagic Fish*. Checkley DM, Alheit J, Oozeki Y (Eds.) (Cambridge University Press, Cambridge), pp. 285-299.

8. Baumgartner T, Soutar A, Ferreira-bartrina V (1992) Reconstruction of the History of Pacific Sardine and Northern Anchovy Populations Over the Past 2 Millennia from Sediments of the Santa-Barbara Basin. *CalCOFI Rep* 33:24-40.

9. Sugihara G, et al. (2012) Detecting Causality in Complex Ecosystems. *Science* 338:496-500.

10. Rykaczewski RR, Checkley DM (2008) Influence of ocean winds on the pelagic ecosystem in, upwelling regions. *Proc Natl Acad Sci USA* 105:1965-1970.

11. van der Lingen CD, Hutchings L, Field JG (2006) Comparative trophodynamics of anchovy *Engraulis encrasicolus* and sardine *Sardinops sagax* in the southern Benguela: are species alternations between small pelagic fish trophodynamically mediated? *Afr J Mar Sci* 28:465-477.

12. Lasker R, MacCall AD (1983) in *Proceedings of the Joint Oceanographic assembly 1982 - General Symposia* (Scientific Committee on Oceanic Research, Ottawa), pp. 110-120.

13. Butler J, Pickett J (1988) Age-specific vulnerability of Pacific sardine, *Sardinops sagax*, larvae to predation by northern anchovy, *Engraulis mordax*. *Fish Bull* 86:163-167.

14. McEvoy AF (1986) *The fisherman's problem. Ecology and law in the California Fisheries 1850-1980.* (Cambridge University Press, New York).

15. Jacobson L, MacCall A (1995) Stock-Recruitment Models for Pacific Sardine (*Sardinops sagax*). *Can J Fish Aquat Sci* 52:566-577.

16. Lindegren M, Checkley DM (2013) Temperature dependence of Pacific sardine (*Sardinops sagax*) recruitment in the California Current revisited and revised. *Can J Fish Aqua Sci* 70:245-252.

17. Fissel BE, Lo NCH, Herrick SF (2011) Daily Egg Production, Spawning Biomass and Recruitment for the Central Subpopulation of Northern Anchovy 1981-2009. *CalCOFI Rep* 52: 116-135.

18. Hastie T, Tibshirani R (1990) *Generalized additive models.* (Chapman and Hall, London).

19. Wood SN (2006) *Generalized additive models. An introduction to R.* (Chapman & Hall/CRC, Boca Raton).

20. Checkley DM, et al. (2009) *in: Climate Change and Small Pelagic Fish*. Checkley DM, Alheit J, Oozeki Y (Eds.) (Cambridge University Press, Cambridge), pp. 14-18.

21. Lynn R (2003) Variability in the spawning habitat of Pacific sardine (*Sardinops sagax*) off southern and central California. *Fish Oceanogr* 12:541-553.

22. Reiss CS, Checkley DM, Bograd SJ (2008) Remotely sensed spawning habitat of Pacific sardine (*Sardinops sagax*) and Northern anchovy (*Engraulis mordax*) within the California Current. *Fish Oceanogr* 17:126-136.

23. Wood SN (2003) Thin plate regression splines. *J R Stat Soc B* 65:95-114.

24. Picard RR, Cook RD (1984) Cross-validation of regression models. *J Am Stat Assoc* 79: 575-583.

25. Steele JH (1985) A Comparison of Terrestrial and Marine Ecological Systems. *Nature* 313:355-358.

26. Halley J (1996) Ecology, evolution and 1/f-noise. *Trends in Ecology & Evolution* 11:33-37.

27. Vasseur D, Yodzis P (2004) The color of environmental noise. *Ecology* 85:1146-1152.

28. Rouyer T, Fromentin J, Stenseth NC, Cazelles B (2008) Analysing multiple time series and extending significance testing in wavelet analysis. *Mar Ecol Prog Ser* 359:11-23.

29. Smith T, Reynolds R, Peterson T, Lawrimore J (2008) Improvements to NOAA's historical merged land-ocean surface temperature analysis (1880–2006). *J Climate* 21: 2283–2296.

30. Field DB, et al. (2009) *in: Climate Change and Small Pelagic Fish*. Checkley DM, Alheit J, Oozeki Y (Eds.) (Cambridge University Press, Cambridge), pp. 45-63.

31. Gedalof Z, Smith D (2001) Interdecadal climate variability and regime-scale shifts in pacific north america. *Geophys Res Lett* 28:1515-1518.

32. D'Arrigo R, Villalba R, Wiles G (2001) Tree-ring estimates of pacific decadal climate variability. *Clim Dyn* 18:219-224.

33. MacDonald G, Case R (2005) Variations in the pacific decadal oscillation over the past millennium. *Geophys Res Lett* 32:L08703.

34. D'Arrigo R, Wilson R (2006) On the asian expression of the PDO. *Int J Climatol* 26:1607-1617.

35. Biondi F, Gershunov A, Cayan D (2001) North Pacific decadal climate variability since 1661. *J Clim* 14:5-10.

36. Shen C, Wang W, Gong W & Hao Z (2006) A pacific decadal oscillation record since 1470 AD reconstructed from proxy data of summer rainfall over eastern china. *Geophys Res Lett* 33:L03702.

37. Benjamini Y, Hochberg Y (1995) Controlling the false discovery rate: a practical and powerful approach to multiple testing. *J R Stat Soc B* 57:289–300.